Optics and Lasers in Engineering 49 (2011) 668–674

Contents lists available at ScienceDirect

Optics and Lasers in Engineering

journal homepage: www.elsevier.com/locate/optlaseng

Optical absorption spectroscopy of one-dimensional silicon nanostructures

N. Arzate [a,*], R.A. Vázquez-Nava [a], J.L. Cabellos [a], R. Carriles [a], E. Castro-Camus [a], M.E. Figueroa-Delgadillo [b], B.S. Mendoza [a]

[a] Centro de Investigaciones en Óptica, A.C., León, Guanajuato, México
[b] Unidad Académica de Física, Universidad de Zacatecas, Zacatecas, México

ARTICLE INFO

Available online 8 January 2011

Keywords:
Silicon nanostructures
Optical techniques
Absorption spectroscopy

ABSTRACT

During the last decade there has been a great development in nanoscience and nanotechnology. The technology of nanostructures synthesis and characterization has grown rapidly and optical spectroscopy has become a very useful characterization technique, since it provides information on the structural, electronic, optical and dynamical properties of materials. Nanostructures have unique physical properties that are different from bulk materials. A wealth of interesting and new phenomena are associated with nanometer-sized structures, such as size-dependent emission or excitation, metallic and semiconductor behavior, etc. Here we present an overview of the linear optical response of one-dimensional silicon nanostructures. In particular, we make a theoretical study of the effects of the size and shape of one-dimensional silicon structures on the absorption spectrum, focusing on the calculation of the linear optical response of clean and hydrogen-adsorbed armchair (6,6) silicon nanotubes. We discuss the changes of the absorption spectrum of silicon nanowires with different diameters and analyze the behavior of the band gap as we go from bulk silicon to one-dimensional silicon nanostructures with nanometer-size diameters.

1. Introduction

The continued progress of technology in the miniaturization of different kinds of atomic structures has led to the fabrication of novel structures with nanometer scale called nanostructures. The physical properties of nanostructures are significantly different from those of their bulk counterparts. For instance, there is an enhancement of the mechanical strength, the optical absorption peak shifts to a shorter wavelength due to an increase in the band gap, the color of metallic nanoparticles may change due to surface plasmon resonance, nanotubes (NTs) can either be metallic or semiconducting depending of their chirality, the electrical conductivity of nanomaterials could be enhanced appreciably, etc. In general, the physical properties of nanostructures depend on their size and shape. If the carriers, electrons and holes, are confined to dimensions less than their de Broglie wavelength (typically few nanometers), quantum-mechanical size effects become important. Bulk silicon, for instance, has a relatively small and an indirect band gap, thus it emits a weak infrared photoluminescence. In indirect semiconductors the crystal momentum is not conserved during relevant transitions, which, under normal circumstances, prevents efficient interband radiative recombination. However, it was found that one-dimensional structures of highly porous silicon emit efficiently under photoexcitation due to quantum-size effects [1,2]. Depending on the degrees of freedom, the carrier confinement can be zero-dimensional, such as in quantum dots, one-dimensional, such as in nanowires (NWs), or two-dimensional, such as in quantum wells.

The discovery of carbon NTs [3,4] increased the interest in one-dimensional nanostructures, such as NTs and NWs, due to their novel properties. These nanostructures are expected to play a key role in a variety of applications such as optoelectronics, photonics, biotechnology, etc. Hence, knowledge of their atomic and electronic structure is a main issue in order to control and understand their electronic behavior and properties. Both theoretical and experimental studies of one-dimensional nanostructures are still challenging problems. Among the different kinds of studied nanostructures, silicon nanostructures are technologically interesting, since it is the fundamental material of use in electronics, and thus they would have better compatibility with present silicon technology. We refer the reader to the review of silicon nanotechnology published by Teo and Sun [5], wherein particular attention is paid to the building of silicon-based low-dimensional nanomaterials, the manipulating techniques and nanodevice fabrication.

Here we present a theoretical study of the effects of the size and the shape of one-dimensional silicon structures on the absorption spectrum. In particular, we calculate the linear optical response of clean and hydrogen-adsorbed armchair (6,6) silicon NTs. We discuss our results along with the corresponding spectra of silicon NWs with different diameters. We also focus on the tailoring of the

* Corresponding author.
E-mail address: narzate@cio.mx (N. Arzate).

0143-8166/$ - see front matter © 2010 Elsevier Ltd. All rights reserved.
doi:10.1016/j.optlaseng.2010.12.007

band gap as we go from bulk silicon to one-dimensional silicon nanostructures with nanometer-size diameters. The organization of the paper is as follows. In Section 2, we give a brief overview of the different experimental and theoretical studies on one-dimensional silicon nanostructures with emphasis on silicon NTs along with their structural characteristics. We explain, in Section 3, the modeling of NTs and the methodology employed for the calculations performed on this work for their linear optical response. In Section 4, we show the corresponding absorption spectra, through spectra of the imaginary part of the dielectric function, for clean and hydrogen-adsorbed silicon NTs. We also give a discussion of the calculations of this work with those performed on hydrogen-adsorbed silicon NWs. Finally, in Section 5, we give conclusions.

2. One-dimensional silicon nanostructures

Silicon crystallizes in a diamond-like structure forming covalent σ bonds in tetragonal coordination also known as sp^3 hybridization. The formation of more stable hybridized sp^3 bonds in silicon leads to fourfold coordination with four equivalent directions for growth. This gives a reason why silicon nanostructures with bulk-like core are more favorable than hollow structures. Dealing with one-dimensional nanostructures, the sp^3 hybridization favors the formation of silicon NWs rather than silicon NTs. This is in contrast to carbon, which can form strong π bonds through sp^2 hybridization, spanning a variety of forms such as graphite, fullerenes, NTs, etc. This is better explained as follows [5]: the larger atomic size of silicon gives rise to longer and weaker silicon–silicon bonds with lengths of 2.35 Å and bond energies of 222 kJ/mol, in comparison to carbon–carbon bonds of length of 1.54 Å and bond energy of 345.6 kJ/mol. As a result covalent silicon bonds are often non-planar. Besides the energy difference between the valence s and p orbitals for silicon is only half of the corresponding value of carbon. As a result, silicon tends to utilize all three of its valence p orbitals, resulting in a sp^3 hybridization, in contrast to carbon, which can activate one valence p orbital at a time to give sp, sp^2 and sp^3 hybridizations.

Studies on NWs show that, for diameters over 5 nm, silicon NWs often consist of diamond cores surrounded by an oxide layer [6]. Silicon is very easily oxidized, because the diamond-type crystal structure leads to a high density of dangling bonds at the surface. In most studies of silicon nanoparticles and NWs the dangling surface states were passivated. This leads to nanostructures with a crystalline silicon core surrounded by an amorphous silicon oxide layer. For instance, Morales and Lieber reported a method for the synthesis of silicon and germanium NWs [6]. They combined laser ablation cluster formation and vapor–liquid–solid growth to prepare nanometer-diameter catalyst clusters. They prepared bulk quantities of uniform single-crystal silicon and germanium NWs with diameters ranging from 6 to 20 and from 3 to 9 nm, respectively, and lengths ranging from 1 to 30 μm. Later, Marsen and Sattler reported the formation of oxide-free silicon NWs grown from the atomic vapor in ultra high vacuum. The diameter of the wires ranged from 3 to 7 nm and the length was at least 100 nm. They tend to be assembled parallel in bundles [7]. Ma et al. [8] also reported small diameter silicon NWs with diameters of 1.2–7 nm, from which the oxide sheath was removed and whose surfaces were terminated with hydrogen.

On the other hand, the synthesis of hollow one-dimensional silicon nanostructures has been difficult to achieve due to the sp^3 hybridization of silicon instead of the sp^2 hybridization shown in graphite. However, the synthesis of silicon NTs has been possible to achieve from silicon monoxide and by using the method of self-assembling [9,10]. The structures of the silicon NTs were hollow inner pore, crystalline silicon wall layers with a 0.31 nm interplanar spacing and 23 nm amorphous silica outer layers. These amorphous silica outer layers were later removed by an etching process. The diffraction rings matched well with the 111 and 220 diffraction rings of silicon. Silicon NTs have also been prepared by chemical vapor deposition (CVD) using a nanochannel Al_2O_3 substrate [11], and molecular beam epitaxy (MBE) using porous alumina templates [12], wherein the NTs had diameters of around 50 nm. In the latter case the nanotube wall thickness was of 4–5 nm. Furthermore, De Crescenzi et al. [13] reported the synthesis of clean silicon tubes by dc-arc plasma method. They obtained NTs, which had diameters ranging from 2 to 35 nm and observed that the silicon NTs were organized in a honeycomb lattice and conclude that they form a puckered lattice. Menon and Richter [14] used a generalized tight-binding molecular-dynamics scheme and showed that one-dimensional structures can be stable provided that their geometries consist of a core of fourfold-coordinated atoms, surrounded by a threefold-coordinated outer surface incorporating one of the most stable reconstructions of bulk silicon. Later Fagan et al. [15] examined the electronic and structural properties of hypothetical silicon NTs through first-principles calculations based on density functional theory (DFT). The considered NTs were formed in the same way as the carbon NTs. They showed that, similar to carbon structures, depending on their chiralities, silicon NTs may present metallic or semiconductor behaviors: the armchair NTs are metallic and all other NTs are semiconducting. Kumar et al. [16] performed *ab initio* calculations of silicon fullerenes. They stated that adsorption of hydrogen on the silicon fullerenes enhances sp^3 bonding between the silicon atoms, making the fullerenes, with adsorption of only hydrogen atoms, stable. They found large highest occupied and lowest unoccupied molecular orbital gaps of 2.5–3.0 eV.

Another atomistic computer-simulation study on the possible existence of one-dimensional silicon nanostructures was done by Bai et al. [17] They considered square, pentagonal, and hexagonal single-walled (SW) silicon NTs. The local geometric structure of the SW silicon nanotube (NT) differs from the local tetrahedral structure of cubic diamond silicon, although the coordination number of atoms of the SW silicon NTs is still fourfold. Their *ab initio* calculations showed that SW silicon NTs are locally stable in vacuum at zero temperature and have zero band gap, suggesting that the SW silicon NTs are possibly metals rather than wide-gap semiconductors. A unique structural feature of these SW silicon NTs is that the coordination number of every silicon atom is fourfold, which differs from that of SW carbon NTs. Starting from precursor graphene-like structures, the stability and electronic structure of zigzag and armchair tubes, using *ab initio* calculations, were investigated by Durgun et al. [18] They showed that $(n,0)$ zigzag and (n,n) armchair silicon NTs, with $n \geq 6$, are stable, but those with $n \leq 6$ can be stabilized by internal or external adsorption of transition metal elements. Stable $(n,0)$ zigzag SW silicon NTs are metallic for $6 \leq n \leq 11$, but become semiconducting for $n \geq 12$. On the other hand, stable armchair (n,n) SW silicon NTs, with $n=6,9$ are also metallic. Barnard and Russo [19] also performed *ab initio* calculations on smooth-walled silicon NTs and showed that the atomic heat of formation of a silicon NT is dependent on its diameter, but independent of the chirality of the tube. They also showed that the individual cohesive and strain energies are dependent on both the diameter and the chirality of the tubes.

Seifert et al. [20] consider silicides and SiH as precursors of possible silicon-based NTs. The silicon layers in the silicides are not ideally planar as in graphene but become puckered. Seifert et al. obtained the structure, energetics, electronic and mechanical properties of silicide and SiH NTs by using a density-functional tight-binding scheme. They concluded that these NTs are, energetically, highly favorable structures. They proposed to avoid the problem of the dangling bonds for threefold-coordinated silicon in tubular structures by charging or saturating with hydrogen the

silicon NTs. For silicide and SiH NTs, they found that the band gap grows towards the silicide and SiH sheet as the tube diameter is increased. The opposite behavior is observed for silicon NTs adsorbed with hydrogen atoms on the exterior surface of the tube, *i.e.* the band gap decreases towards the respective value of SiH sheet. Zhang et al. [21] showed computationally that SW silicon NTs can adopt a number of distorted tubular structures, representing respective local energy minimum, depending on the theory used and the initial models adopted. In particular, gear-like structures containing alternating sp^3-like and sp^2-like silicon local configurations have been found to be the dominant structural form for silicon NTs via density-functional tight-binding molecular-dynamics simulations at moderate temperatures (below 100 K). The gear-like structures of silicon NTs are energetically more stable than the smooth-walled tubes. They are, however, energetically less favorable than the string-bean-like silicon NT structures, *i.e.* NTs with a string-bean distortion or periodically varying diameter. The energetics and the structures of gear-like silicon NTs are shown to be dependent on the diameter of the tube irrespective of the type of the NT. Meanwhile, the band gap was shown to be sensitive to both the diameter and the type of the NT.

First-principles calculations of silicon NTs showing faceted-wall surfaces have been also performed [17,22]. Bai et al. [17] reported the structural characteristics, bonding modes, and electronic properties of single-crystalline silicon NTs. They found that pristine silicon NTs with sp^3 hybridization constructed by the bulk-like tetrahedrally coordinated silicon atoms are energetically stable. The electronic properties are sensitive to the external diameter, tube-wall thickness, and tube-axis orientation due to quantum confinement effects. A direct band gap is observed in silicon NTs with smaller sizes. The band gap increases monotonically with decreasing tube-wall thickness, in agreement with the substantial blueshift observed in the experiment. On the other hand, Zhao et al. [22] reported configurations of double-walled silicon NTs with faceted-wall surfaces that have higher energetic favorability than the conventionally adopted cylindrical configurations of SW silicon NTs. They showed that hexagonal- and tetrahedral-like structures of these double-wall silicon NTs are almost energetically equivalent, since they have very close formation energies, but they show quite different electronic structures.

3. Method

We present *ab initio* calculations for the absorption or imaginary part of the dielectric function of clean and hydrogen-adsorbed SW silicon NTs. In order to calculate the dielectric function of the NTs we follow the method described in Ref. [23]. The type of silicon NT that we study is the armchair (6,6) tube. According to molecular-dynamics simulations performed by Zhang et al., this type of silicon NT is stable. Zhang et al. [21] found in their simulations that silicon NTs, at 0 K, deviate slightly from the smooth-walled structures analogous to those of carbon NTs. However, when the temperature rise to 10–30 K, structural deformation can occur. In particular, small diameter zigzag silicon NTs, for $n < 6$, easily collapse in the temperature range of 10–30 K. Silicon NTs with larger diameters can usually withstand higher temperatures in the annealing process. Indeed, the armchair (6,6) NT with a diameter value of 1.24 nm satisfies this condition.

We have used an *ab initio* method in order to determine the relaxed atomic arrangement of the silicon tubular structures and obtain the optical-response spectrum. The method is based on the framework of Kohn–Sham DFT within the local density approximation (LDA) and the many-body perturbation method based on the GW approximation, focusing on the GW band gap correction. The calculations have been obtained using the ABINIT code [24–26], that is based on pseudopotentials and plane waves. The ionic-core potential was replaced by a separable dual-space Gaussian pseudopotential [27] and a plane-wave energy cutoff of 20 Ha was used. Spin–orbit interaction was not considered in the calculation. It is well known that DFT has been successful for describing ground-state properties, such as total energies and structural properties. However, DFT underestimates the band gaps of semiconductors, since the single-particle hamiltonian cannot describe accurately the actual eigenvalues of the many-body hamiltonian. The Green function method (GW), that is suitable to study excited-state properties of extended systems, is a many-body approximation that corrects such an inaccuracy [28–30]. Here we incorporate this many-body effect at the level of the GW-scissors band gap correction.

Recent calculations have shown that the inclusion of local-field effects (LFE) are important to fully interpret the experimental absorption spectra of NTs [31,32], and NWs [33,34]. Therefore, in these kind of systems, it is important to take into account the induced microscopic components in the response to the external field; as a result a so-called depolarization effect takes place for the perpendicular polarization of the field to the nanostructure surface. The self-consistency between the total perturbing potential and the charge response induces Hartree and exchange-correlation potentials giving rise to many-body and excitonic effects respectively. Both GW approach [28,30] and the time dependent DFT method [35,36] can include such effects. In the former, electron self-energy corrections to the DFT Kohn–Sham band structure are considered and the electron-hole interaction is described by the Bethe–Salpeter equation. In the latter, the many-body effects are embodied in the exchange-correlation potential, and it offers the important practical advantage of a dependence on density rather than on multivariate Green's functions [37]. The time-dependent DFT calculation of the optical absorption of NTs is almost unaltered with the inclusion of LFE [31,32], for light polarized parallel to the NT axis. In contrast, in the case of perpendicular polarization of the field, the absorption of the light at lower energies is suppressed. Hence, the corresponding GW calculation, at the level of the scissors correction to the band gap, and for light polarized parallel to the NT axis, must only shift the absorption spectrum to higher frequencies.

4. Results

Firstly, we have performed an optimization of the bulk silicon structure through minimization of the total energy, where we calculated the values of 5.39 and 2.34 Å, for the lattice constant and silicon–silicon bond length, respectively, which are in good agreement with the experimental values of 5.43 and 2.35, respectively. Then, we performed the total energy minimization of a Si(1 1 1) layer structure, wherein the values of 3.74 Å and 2.30 for the lattice constant and silicon–silicon bond length, respectively, were found. Our calculated value for the lattice constant of the Si(1 1 1) layer is comparable to that of 3.75 Å calculated by Yan and Ni [38]. Hence, initial configurations of the NTs were constructed by folding such a two-dimensional puckered Si(1 1 1) layer. On the other hand, the hydrogen-adsorbed NT was formed by considering a Si(1 1 1) sheet with all their dangling bonds saturated by hydrogen above and below the layer. Once the clean and hydrogen-adsorbed Si(1 1 1) layers are folded, ideal NT structures are formed, which show a non-smooth wall as they are shown in Fig. 1. In order to model the NT structure, a supercell geometry was formed in such a way that there would be NTs aligned in a square array with a distance between NTs of at least 23 Å. Then, the underlying nanotube-structure was obtained through a full relaxation of the atomic positions to its ground state. The equilibrium structures were

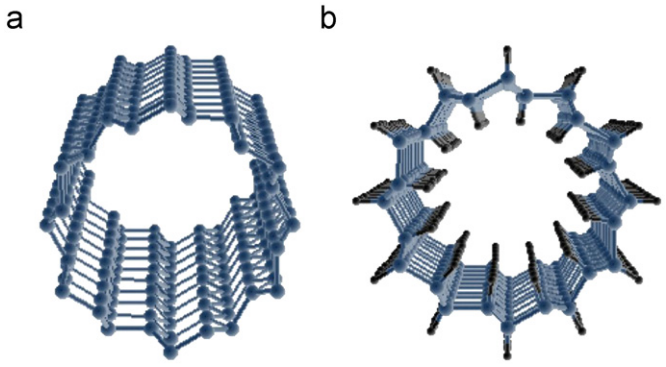

Fig. 1. Front views of the clean (a) and hydrogen-adsorbed (b) armchair silicon (6,6) NTs. The hydrogen atoms bind to the dangling bonds at the surface of the NT.

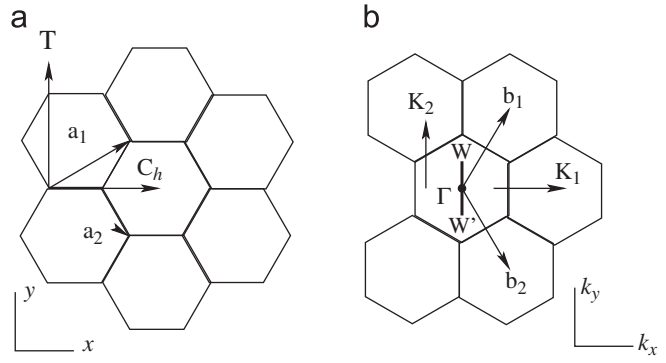

Fig. 2. Schematic diagrams showing the real (a) and reciprocal (b) lattices of an armchair NT. On the figure, $\mathbf{a}_1$ and $\mathbf{a}_2$ are the unit lattice vectors of the two-dimensional graphene-like sheet; meanwhile $\mathbf{b}_1$ and $\mathbf{b}_2$ are the corresponding reciprocal lattice vectors. The arrow $\mathbf{C}_h$ indicates the direction of the chiral vector and the arrow **T** indicates the direction of the translational vector. Those vectors define the unit cell of the NT; Similarly, the arrows for $\mathbf{K}_1$ and $\mathbf{K}_2$ indicate the directions for the corresponding reciprocal lattice vectors. The line segment WW′, which is parallel to $\mathbf{K}_2$ or to the NT axis, represents the one-dimensional Brillouin zone of the NT.

obtained when the forces acting on the atoms were less than 0.003 eV/Å. The optimized axial lattice constant or translational vector length of the NT found was of 7.18 Å. Besides, the average silicon–silicon bond lengths, for the clean NT, resulting from the relaxation was 2.26 Å, which is comparable to that found by other authors [15,19,39]. Meanwhile, the optimized axial lattice constant of the hydrogen-adsorbed silicon NT has the value of 7.23 Å and their silicon–silicon and silicon–hydrogen bonds lengths have the average values of 2.33 and 1.51 Å, respectively. We also mention that the obtained optimized NT structures contain two alternating silicon sites, A and B, just as the study of Zhang states [21]. The site A is close to tetrahedral characteristic of a sp^3-like hybridization, while the site B is approximately trigonal planar characteristic of a sp^2-like hybridization.

On the evaluation of the linear optical response, we calculate the dielectric function within the independent particle approximation and use the linear analytical tetrahedron method [41]. The energy eigenvalues and matrix elements were calculated at 20 **k** points in the irreducible Brillouin zone (BZ), which were uniformly distributed along the NT axis, and 150 conduction bands were used. Finally, we have chosen the effective unit cell volume of the NT employed in Ref. [42], with a NT wall thickness equal to the interlayer distance of two equivalents layers of the (1 1 1) silicon surface.

Fig. 2 shows the real and reciprocal lattices of the armchair NT, along with the real and reciprocal vectors of both the two-dimensional graphene-like sheet and the armchair tube. We then show, in Fig. 3, the energy bands for both the clean (a) and hydrogen-adsorbed (b) armchair (6,6) silicon NTs. The clean tube shows to be a semiconductor with a direct band gap of 1.19 eV, close to the indirect band gap of bulk silicon. The GW-scissors correction to the band gap is 0.77 eV. Meanwhile, the hydrogen-adsorbed NT shows to have a wide band gap with a value of 5.33 eV and GW-scissors correction value of 3.33 eV. Table 1 tabulates the band gaps for the studied NTs along with three nanowire (NW) configurations.

Fig. 4 shows the calculated spectra for the imaginary part of the dielectric function for the following structures: bulk silicon,

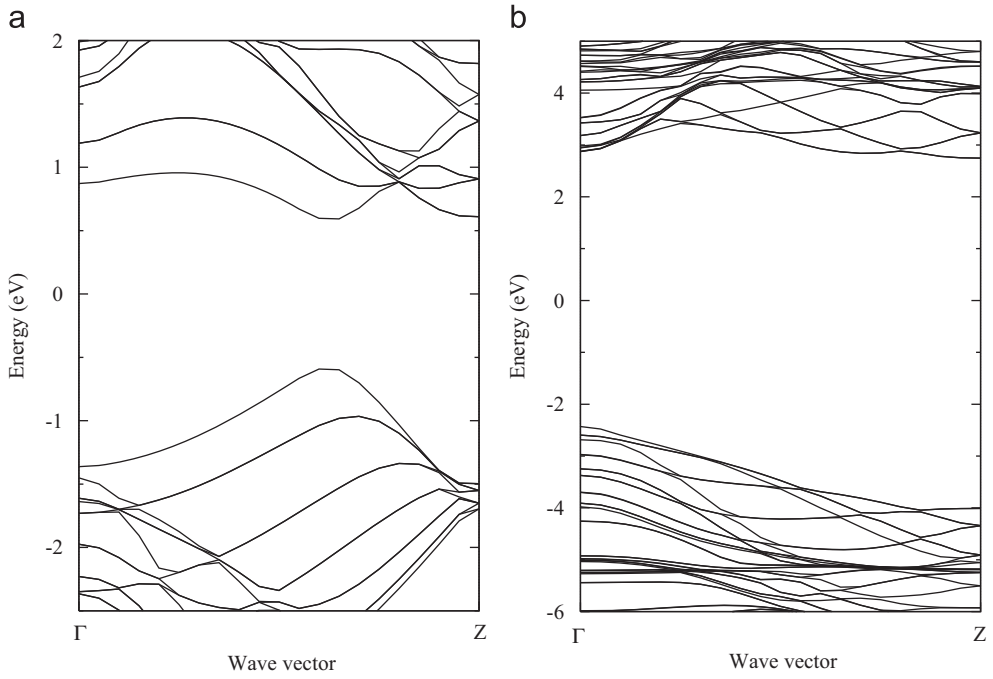

Fig. 3. Energy band structures of the clean (a) and hydrogen-adsorbed (b) armchair (6,6) silicon NTs. The Fermi level is at 0 eV and the wave-vector-path, Γ–Z, is along the direction of the reciprocal lattice vector $\mathbf{K}_2$ of the NT (see Fig. 2), being $Z=\pi/T$, with T the length of the translational vector [40].

Table 1
LDA (E_g^{LDA}) and GW (E_g^{GW}) band gaps of one-dimensional silicon nanostructures analyzed in this work. The corresponding experimental band gap of bulk silicon is 1.17 eV. D is the diameter of the one-dimensional nanostructure, N_{Si} and N_H are the corresponding number of silicon and hydrogen atoms in the considered supercell of the nanostructure. The NWs passivated with hydrogen atoms (NW–H) are wires oriented along the [1 1 0] direction. Their corresponding band gaps values were reported in Ref. [43]. Meanwhile energy band gaps for bulk silicon and NTs were calculated in the present work.

Structure	D (nm)	N_{Si}	N_H	E_g^{LDA}	E_g^{GW} (eV)
Bulk				0.48	1.32
NW–H	2.2	76	28	0.9	1.85
NW–H	1.6	42	20	1.03	2.32
NW–H	1.2	16	12	1.5	3.12
(6,6) NT–H	1.2	24	24	2.0	5.33
Clean (6,6) NT	1.2	24	0	0.42	1.19

hydrogen-passivated silicon NWs with bulk-like structure in their interior and diameters of 2.2 and 1.2 nm, and the clean and hydrogen-adsorbed armchair (6,6) silicon NTs. Fig. 4(a) shows both the experimental (dashed line) and the calculated (solid line) absorption spectra for bulk silicon, wherein we found a GW band gap value of 1.32 eV, with a scissors correction of 0.84 eV. The spectra shown in panels (b)–(e) of Fig. 4 correspond to one-dimensional structures, NWs and NTs; the electric field, for these cases, is polarized along the axial axis of the one-dimensional nanostructure. We can see from Fig. 4(b) and (c) that hydrogen-passivated silicon NWs have a band gap greater than that of bulk silicon, the larger band gap corresponding to the smaller diameter NW. This behavior has been found by other authors [8,43], the smaller the diameter of the NW, the bigger the band gap. The main peak at 4.3 eV for bulk silicon shifts upwards in frequency, remaining approximately 3.0 eV above the corresponding GW band gap value, E_g, in the NWs. Although these NWs structures have a direct fundamental gap, their absorption is vanishingly small near the gap [43], but their absorption edge, where the spectrum becomes appreciably non-zero, is closer to the band gap as the diameter of the NW decreases. This was explained by Zhao et al. as a consequence of mixing the bulk states in finite-sized wires, leading to an enhancement of the dipole transition and giving rise to other lower energy peaks for smaller-diameter wires.

On the other hand, on the study of NTs, it has been found that their electronic properties are quiet different from their bulk counterparts. Since the studied SW silicon NT was formed by rolling a (1 1 1) silicon layer, it is then only composed by both the interior and the exterior surfaces of the tube, wherein each silicon atom on the surface contains a dangling bond. The effect of passivation of the silicon NT has been explored by saturating these dangling bonds with hydrogen atoms on both surfaces. We recall that the (6,6) hydrogen terminated NT has a diameter of 1.24 nm, which is approximately equal to that of the silicon NW considered in Fig. 4(c), but with a hollow core. The corresponding spectrum for the imaginary part of the dielectric function is shown in Fig. 4(d). The adsorption of hydrogen on the surface of the nanotube makes the band gap be quiet large and the absorption edge be near the band gap value. The absorption spectrum show a main peak at around 7.0 eV, and smaller ones at around 5.6 and 6.2 eV, which could be related to the mixing of the sp^3 hybridization, characteristic of a bulk tetrahedral atomic structure, and sp^2 hybridization since the dangling bonds were all saturated. We have also considered the case where the dangling bonds are saturated by hydrogen atoms, only on the exterior surface of the NT. We found that such a structure shows a metallic behavior.

Finally, Fig. 4(e) shows the corresponding dielectric function spectrum for the clean armchair (6,6) silicon SW NT. We firstly see

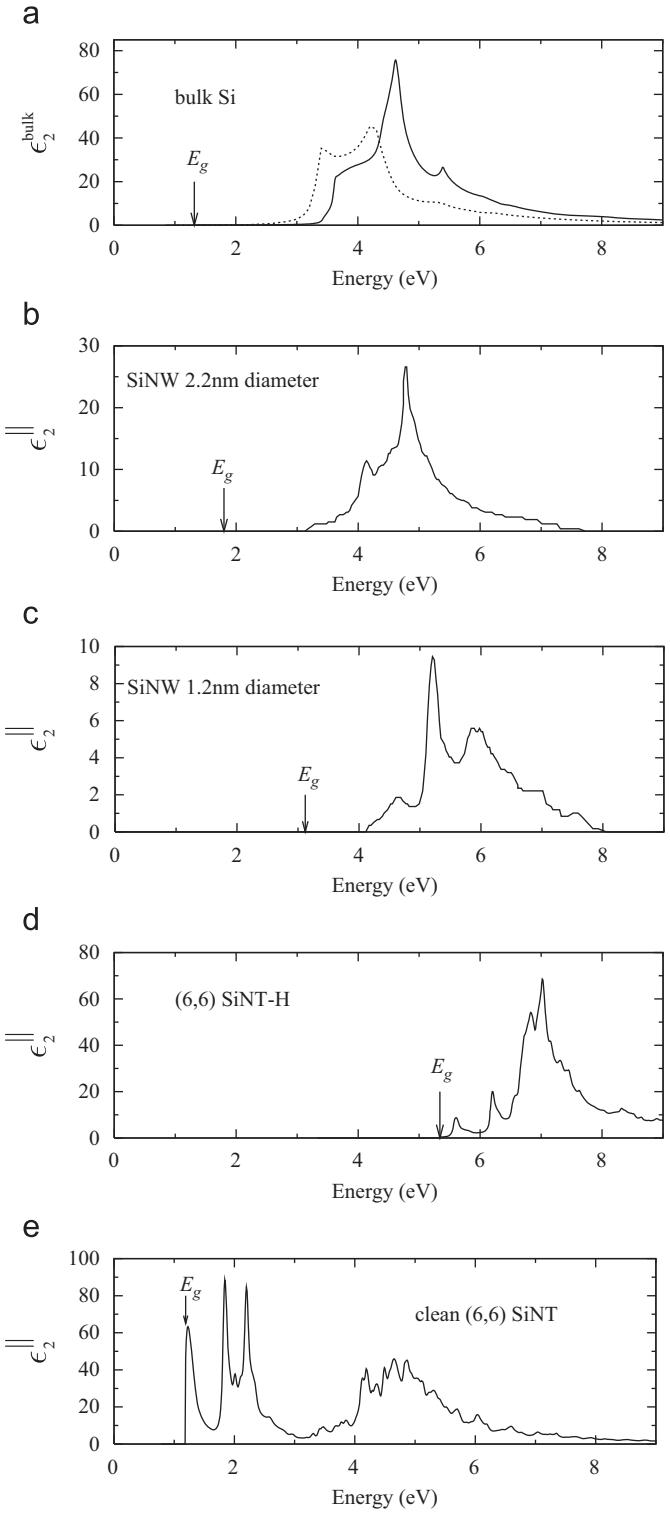

Fig. 4. Spectra for the imaginary part of the dielectric function for the structures: (a) bulk silicon (theoretical-solid line- and experimental [44]-dashed line-spectra), (b) and (c) hydrogen-passivated silicon NWs with 2.2 and 1.2 nm of diameter, respectively (spectra taken from Ref. [43]), (d) and (e) hydrogen-adsorbed and clean armchair (6,6) silicon NT correspondingly. The arrows mark the corresponding GW band gap energies, E_g.

that the respective band gap has a value of 1.19 eV, close to the corresponding bulk value. We also observe that the absorption edge of the spectrum is just above the band gap and that it shows three well defined peaks near the band gap value: at 1.19, 1.86 and 2.21 eV. These peaks are not shown in the corresponding bulk

spectrum and could be related to the presence of mainly surface states or dangling bonds. Furthermore, the wide structure seen above 4 eV might be interpreted as bulk-related since there is a mixing of the sp^3 and sp^2 hybridization of the bonds.

5. Conclusions

Photoluminescence measurements [45] have shown that there is a spectral blueshift as well as an increase of the energy band gap [8] with decreasing diameter of silicon NWs, that are attributed to quantum confinement effects. Such an increase of the energy band gap has been observed by first-principles calculations [43] performed for NWs passivated with hydrogen.

We report in the present work that as the diameter of the silicon NWs passivated with hydrogen decreases and its core becomes hollow, forming a hydrogen-passivated SW NT, the observed spectral blueshift in the absorption spectrum is greater in NTs. In addition, when there is no adsorption of hydrogen, *i.e.* for the clean NTs, there is an appearance of surface states well below the main absorption structure for bulk silicon. Multiple wall NTs with puckered structure could also be considered, wherein the influence of the wall thickness on the absorption spectra can be studied. This is an issue of future work for us. Works related to the electronic structure of multiple wall NTs can be found in Refs. [22,46]. In particular, Yan et al. [46] state that, in general, in the case of single-crystalline silicon NTs, quantum confinement effects along the circumferential and radial directions are related to three-structural parameters: the external diameter of the NT, tube-wall thickness, and tube-axis orientation. In their study, they found that the band-gap character (*i.e.* direct or indirect) is related to the tube external diameter, but is insensitive to the tube-wall thickness. Meanwhile, the band gap increases as the tube-wall thickness decreases and it is insensitive to the external diameter.

Thus optical spectroscopy, in particular the absorption technique, is very useful to characterize nanostructures since, it provides information of their structural and electronic properties. For instance, the line shape of the absorption spectrum gives a signature of the different configurations of the nanostructures. Furthermore, it can be used as a tool to build different types of one-dimensional silicon nanostructures in order to tailor the band gap. As a final remark, we note that, according with our results, partial hydrogenation of the NTs can be considered to tailor the band gap on an ample range in energy by controlling the adsorption of hydrogen coverage on the silicon NT.

Summarizing we have performed *ab initio* pseudopotential calculations of the absorption spectra of clean and hydrogen-adsorbed armchair (6,6) silicon NTs. The armchair (6,6) tube, with diameter of 12.38 Å, is semiconductor showing a band gap of 1.19 eV. Meanwhile, the hydrogen-adsorbed NT has a wide band gap with value of 5.33 eV. The adsorption of hydrogen on the silicon NT significantly change the electronic structure and, thus, the line shape of the absorption spectrum.

The knowledge of the physical effects as well as the chemical and electronic structure of silicon nanostructures is still under development. Both theoretical and experimental studies are still necessary in order to have a better understanding of the formation and the physical behavior of stable one-dimensional silicon nanostructures.

References

[1] Canham L. Silicon quantum wire array fabrication by electrochemical and chemical dissolution of wafers. Appl Phys Lett 1990;57:1046–8.

[2] Cullis A, Canham L. Visible light emission due to quantum size effects in highly porous crystalline silicon. Nature 1991;353:335–8.

[3] Iijima S. Helical microtubules of graphitic carbon. Nature 1991;354:56–8.

[4] Iijima S, Ichihashi T. Single-shell carbon nanotubes of 1 nm diameter. Nature 1993;363:603–5.

[5] Teo B, Sun X. Silicon-based low-dimensional nanomaterials and nanodevices. Chem Rev 2007;107:1454–532.

[6] Morales A, Lieber C. A laser ablation method for the synthesis of crystalline semiconductor nanowires. Science 1998;279:208–11.

[7] Marsen B, Sattler K. Fullerene-structured nanowires of silicon. Phys Rev B 1999;60:11593–600.

[8] Ma D, Lee C, Au F, Tong S, Lee S. Small diameter silicon nanowire surfaces. Science 2003;299:1874–7.

[9] Tang Y, Pei L, Chen Y, Guo C. Self-assembled silicon nanotubes under supercritically hydrothermal conditions. Phys Rev Lett 2005;95. 116102–4.

[10] Chen Y, Tang Y, Pei L, Guo C. Self-assembled silicon nanotubes grown from silicon monoxide. Adv Mater 2005;17:564–7.

[11] Sha XMJ, Niu J, Xu J, Zhang QYX, Yang D. Silicon nanotubes. Adv Mater 2002;14:1219–21.

[12] Jeong S, Kim J, Yang H, Yoon B, Choi SH, Kang H, et al. Synthesis of silicon nanotubes on porous alumina using molecular beam epitaxy. Adv Mater 2003:1172–6.

[13] Crescenzi MD, Castrucci P, Scarselli M, Diociaiuti M, Chaudhari P, Balasubramanian C, et al. Experimental imaging of silicon nanotubes. Appl Phys Lett 2005;86. 231901–3.

[14] Menon M, Richter E. Are quasi-one dimensional structures of Si stable. Phys Rev Lett 1999;83:792–5.

[15] Fagan S, Baierle R, Mota R, Da Silva A, Fazzio A. Ab initio calculations for a hypothetical material: silicon nanotubes. Phys Rev B 2000;61(15):9994–6.

[16] Kumar V, Kawazoe Y. Hydrogenated silicon fullerenes: effects of H on the stability of metal-encapsulated silicon clusters. Phys Rev Lett 2003;90:055502.

[17] Bai J, Zeng X, Tanaka H, Zeng J. Metallic single-walled silicon nanotubes. Proc Natl Acad Sci USA 2004;101:2664–8.

[18] Durgun E, Tongay S, Ciraci S. Silicon and III–V compound nanotubes: structural and electronic properties. Phys Rev B 2005;72. 075420–10.

[19] Barnard A, Russo S. Structure and energetics of single-walled armchair and zigzag silicon nanotubes. J Phys Chem B 2003;107:7577–81.

[20] Seifert G, Köhler T, Urbassek H, Hernández E, Frauenheim T. Tubular structures of silicon. Phys Rev B 2001;63. 193409–4.

[21] Zhang R, Lee H, Li W, Teo B. Investigation of possible structures of silicon nanotubes via density-functional tight-binding molecular dynamics simulations and ab initio calculations. The J Phys Chem B 2005;109:8605–12.

[22] Zhao M, Zhang R, Xia Y, Song C, Lee S. Faceted silicon nanotubes: structure, energetic, and passivation effects. The J Phys Chem C 2007;111:1234–8.

[23] Arzate N, Vázquez-Nava R, Mejía J, González C, Mendoza B. Linear optical response of nanotubes. In: Espinosa-Luna R, Bernabeu E, Aboites V, editors. Recent Research in Photonics. Research Signpost; 2009. p. 127–51.

[24] The ABINIT code is a common project of the Université Catholique de Louvain, Corning Incorporated, and other contributors, (URL 〈http://www.abinit.org〉).

[25] Gonze X, Beuken J-M, Caracas R, Detraux F, Fuchs M, Rignanese G-M, et al. First-principles computation of material properties: the abinit software project. Comput Mater Sci 2002;25:478–92.

[26] Gonze X, Rignanese G-M, Verstraete M, Beuken J, Poillon Y, Caracas R, et al. A brief introduction to the abinit software package. Z Krystallogr 2005;220:558–62.

[27] Goedecker S, Teter M, Hutter J. Separable dual-space gaussian pseudopotentials. Phys Rev B 1996;54:1703–10.

[28] Hedin L. New method for calculating the one-particle Green's function with application to the electron-gas problem. Phys Rev 1965;139:A796–823.

[29] Hott R. GW-approximation energies and Hartree–Fock bands of semiconductors. Phys Rev B 1991;44:1057–65.

[30] Aryasetiawan F, Gunnarsson O. The GW method. Rep Prog Phys 1998;61:237–312.

[31] Marinopoulos A, Reining L, Rubio A, Vast N. Optical and loss spectra of carbon nanotubes: depolarization effects and intertube interactions. Phys Rev Lett 2003;91. 046402–4.

[32] Marinopoulos A, Wirtz L, Marini A, Olevano V, Rubio A, Reining L. Optical absorption and electron energy loss spectra of carbon and boron nitride nanotubes: a first-principles approach. Appl Phys A 2004;78:1157–67.

[33] Bruneval F, Botti S, Reining L. Comment on quantum confinement and electronic properties of silicon nanowires. Phys Rev Lett 2005;94. 219701–1.

[34] Bruno M, Palummo M, Marini A, Del Sole R, Ossicini S. From Si nanowires to porous silicon: the role of excitonic effects. Phys Rev Lett 2007;98. 036807–4.

[35] Runge E, Gross E. Density-functional theory for time-dependent systems. Phys Rev Lett 1984;52:997–1000.

[36] Dobson F, Petersilka M. Density functional theory. New York: Springer; 1996.

[37] Onida G, Reining L, Rubio A. Electronic excitations: density-functional versus many-body Green's-function approaches. Rev Mod Phys 2002;74:601–59.

[38] Yang X, Ni J. Electronic properties of single-walled silicon nanotubes compared to carbon nanotubes. Phys Rev B 2005;72. 195426–5.

[39] Zhang R, Lee S, Law C, Li W, Teo B. Silicon nanotubes: why not? Chem Phys Lett 2002;364:251–8.

[40] The energy bands of a NT consist of a set of one-dimensional energy dispersion relations, which are cross sections of that of the two-dimensional graphene-like structure. The NT is a structure that is infinite along its axis, but is finite along the chiral vector (see Fig. 2). Therefore the wave vector $\mathbf{k}$ varies continuously in the range $-\pi/T < k < \pi/T$, along the reciprocal lattice vector, $\mathbf{K}_2$, and takes discrete values defined by $\mu\mathbf{K}_1$, with $\mu = 0, \ldots, N-1$, along the reciprocal lattice vector, $\mathbf{K}_1$. N is the number of hexagons on the NT unit cell,

which, in particular, for the armchair (6,6) tube, $N=12$. For a more detailed explanation of the BZ of the NT, see, for instance, Ref. [47].

[41] Moss D, Sipe J, van Driel H. Application of the linear-analytic tetrahedra method of zone integration to nonlinear response functions. Phys Rev B 1987;36:1153–8.

[42] Guo G, Chu K, Wang D, Duan C. Linear and nonlinear optical properties of carbon nanotubes from first principles calculations. Phys Rev B 2004;69. 205416–11.

[43] Zhao X, Wei C, Yang L, Chou M. Quantum confinement and electronic properties of silicon nanowires. Phys Rev Lett 2004;92. 236805–4.

[44] Aspnes DE, Studna AA. Dielectric functions and optical parameters of Si, Ge, GaP, GaAs, GaSb, InP, InAs, and InSb from 1.5 to 6.0 eV. Phys Rev B 1983;27(2):985–1009.

[45] Zhang R, Tang Y, Peng H, Wang N, Lee C, Bello I, Lee S. Diameter modification of silicon nanowires by ambient gas. Appl Phys Lett 1999;75:1842–4.

[46] Yan B, Zhou G, Wu J, Duan W, Gu B. Bonding modes and electronic properties of single-crystalline silicon nanotubes. Phys Rev B 2006;73. 155432–6.

[47] Saito R, Dresselhaus G, Dresselhaus M. Physical properties of carbon nanotubes. Imperial College Press; 1998.